Influence of dephasing on many-body localization

Mariya V. Medvedyeva, Tomaž Prosen, and Marko Žnidarič

Physics Department, Faculty of Mathematics and Physics, University of Ljubljana, SI-1000 Ljubljana, Slovenia

We study the effects of dephasing noise on a prototypical many-body localized system—the XXZ spin 1/2 chain with a disordered magnetic field. At times longer than the inverse dephasing strength the dynamics of the system is described by a probabilistic Markov process on the space of diagonal density matrices, while all off-diagonal elements of the density matrix decay to zero. The generator of the Markovian process is a bond-disordered spin chain. The scaling variable is identified, and independence of relaxation on the interaction strength is demonstrated. We show that purity and von Neumann entropy are extensive, showing no signatures of localization, while the operator space entanglement entropy exhibits a logarithmic growth with time until the final saturation corresponding to localization breakdown, suggesting a many-body localized dynamics of the effective Markov process.

I. INTRODUCTION

Disorder in a noninteracting system in one dimension leads to unavoidable localization of the electron wave functions [1] due to interference, called single particle localization. Naively, interactions between particles could lead to delocalization, and indeed, at small disorder strength the wave functions overlap significantly, leading to thermalization in finite time [2]. For larger disorder strength though the localization prevails—the so-called many-body localization (MBL)—which has been shown to be stable for small interactions [3,4]. The MBL transition can be observed in level spacing statistics [5] as well as in dynamic quantities [6], like a slow logarithmic growth of the entanglement entropy with time [7,8], which is also able to distinguish the MBL and the simpler single particle localized phase. Such MBL behavior can be attributed to the presence of the (quasi)local integrals of motion [9–12] that guarantee a presence of memory effects, in other words, an MBL system is not ergodic [13]. For other interesting properties of MBL systems and a more extensive list of references, see reviews [14,15].

It is important to understand if an MBL phase persists in the presence of an inevitable coupling to external degrees of freedom, for instance, in experiments [16–18] probing MBL, that managed to demonstrate nonergodicity in the presence of controlled interaction and disorder [16]. The influence of an external coupling has been experimentally studied [18,19] with theoretical understanding though still lacking. It is known for instance that Hamiltonian baths will lead to a broadening of spectral functions [20,21]. Similarly, coupling to another clean [22] or disordered [18] system can lead to delocalization. We will in particular focus on an experimentally relevant (and measured [19]) dephasing type of dissipation. Dephasing in general arises due to a coupling that preserves local magnetization (or the particle number, in the fermion language, natural for optical lattice experiments). While such coupling cannot change the occupation of local sites, it can cause a phase difference between occupational states. This can in turn result in the decay of off-diagonal density matrix elements, leading to a phase damping, also called dephasing. Alternatively, a Lindblad equation with dissipation of the dephasing type can be derived when there is a fluctuating external field [23],

or when one performs a continuous measurement of a site occupation [24]. The latter is in fact the case in optical lattice experiments [19] where off-resonant photon scattering effectively "measures" the local site occupation, resulting in dephasing [25]. While it has been shown [26] that dephasing eventually breaks the MBL phase, resulting in diffusion, we shall study how relaxation to this state proceeds. We note that the same problem has been considered recently in Ref. [27], with different scaling on disorder strength predicted. Another topological perspective on the behavior of similar disordered systems under open (dissipative) quantum dynamics has been considered in Ref. [28].

In this paper we treat the quantum dissipative dynamics by perturbation theory in the inverse disorder strength. Such an approach, firstly, provides us with a scaling variable and shows that in one dimension the interactions between particles do not influence the relaxation. Secondly, it reduces the dimension of the Hilbert space for the operators of interest and allows to obtain scaling functions for the time evolution of observables in the thermodynamic limit.

II. THE MODEL

We shall study a prototypical MBL system in the presence of dephasing, described by a Lindblad equation [29] $\frac{\partial \rho}{\partial t} = \mathcal{L}[\rho]$, where

$$\mathcal{L}[\rho] = -i[H,\rho] + \mathcal{D}[\rho], \quad \mathcal{D}[\rho] = \sum_j (2l_j \rho l_j^\dagger - \{l_j^\dagger l_j, \rho\}),$$

$$(1)$$

with Lindblad operators $l_j = \sqrt{\frac{\gamma_j}{2}} \sigma_j^z$. For the derivation see books in Refs. [23,24], or Ref. [25] for the optical lattice context. In MBL experiments [19] the dephasing strength γ_j depends on the laser intensity and detuning. The Hamiltonian is the canonical MBL system, namely the disordered XXZ spin chain,

$$H = \sum_{j=1}^{L-1} J_j \left(\sigma_j^x \sigma_{j+1}^x + \sigma_j^y \sigma_{j+1}^y + \Delta \sigma_j^z \sigma_{j+1}^z \right) + \sum_{j=1}^{L} h_j \sigma_j^z, \quad (2)$$

where L is the number of sites and σ_j^α are Pauli matrices. Note that this model after Jordan-Wigner transformation becomes a spinless Fermionic model, whose spinful version is the subject of cold atomic experiments [16,18]. The magnetic field h_j is random and uniformly distributed in the interval $h_j \in [-2h,2h]$ for some disorder strength h. In this notation the transition from the ergodic to the MBL phase happens [13,30] around $h = h_c \approx 3.7$. We are interested in the influence of the dephasing on the MBL phase, so we focus on $h > h_c$. The steady state (determined by the condition $\mathcal{L}[\rho] = 0$) is an infinite temperature state, $\rho \propto \mathbb{1}$, as can be easily seen from the Lindblad equation.

Effective description. Since the critical field h_c is large, we shall use perturbation theory in the inverse disorder strength h for an effective theoretical description. For not too short times, $t > \max_j(1/\gamma_j)$, the dynamics is governed by eigenvalues of $\mathcal{L}$ that are close to the steady-state eigenvalue 0, and those eigenvalues will be correctly accounted for by our theory. We split the Liouvillian $\mathcal{L}$ into a "large" $\mathcal{L}_0$ that contains the diagonal part in the computational basis (terms with Δ, h_j and γ_j) and $\mathcal{L}_1$ that contains the hopping. Because eigenvalues of $\mathcal{L}_0$ are large compared to those of $\mathcal{L}_1$ the pseudoinverse $\mathcal{L}_0^{-1}$ is uniformly small, resulting in a well behaved perturbation series. Our discussion here closely follows that in Refs. [31,32], where a similar method has been used for clean systems, see also a similar-spirited approach in the context of Rydberg gases [33]. $\mathcal{L}_0$ has a degenerate eigenvalue 0 with eigenoperators being projectors $|\psi_n\rangle\langle\psi_n|$ to all 2^L joint eigenstates $|\psi_n\rangle$ of σ_j^z (*computational basis*). In the first order the degeneracy is not removed (only off-diagonal eigenoperators of $\mathcal{L}_0$ are affected), while the second order degenerate perturbation theory gives

$$\mathcal{L}_{\text{eff}} = -\mathcal{P}\mathcal{L}_1(1-\mathcal{P})\mathcal{L}_0^{-1}(1-\mathcal{P})\mathcal{L}_1\mathcal{P}, \qquad (3)$$

where $\mathcal{P}$ is a projector to the eigenspace of $\mathcal{L}_0$ with eigenvalue 0. Because $\mathcal{L}_{\text{eff}}$ is Hermitian, we write its matrix elements as $[H_{\text{eff}}]_{m,n} := -\text{tr}[|\psi_m\rangle\langle\psi_m|\mathcal{L}_{\text{eff}}(|\psi_n\rangle\langle\psi_n|)]$, resulting in (see Appendix)

$$H_{\text{eff}} \approx \sum_j \frac{2J_j^2(\gamma_j + \gamma_{j+1})}{(h_{j+1} - h_j)^2}(1 - \vec{\sigma}_j \cdot \vec{\sigma}_{j+1}) \qquad (4)$$

where we write explicitly only the leading order (quadratic) terms in $1/h$. From now on we set $J_j \equiv J$ and $\gamma_j \equiv \gamma$. As we shall demonstrate, for times much larger than $1/\gamma$, the dynamics of $\rho(t)$ is correctly described by H_{eff} [34]. Namely, on a time scale $\sim 1/\gamma$ all off-diagonal terms in $\rho(t)$ decay to zero, and what remains for $t > 1/\gamma$ is a process generated by H_{eff} on the linear space spanned by projectors $|\psi_n\rangle\langle\psi_n|$:

$$\rho(t) \approx \sum_n p_n(t)|\psi_n\rangle\langle\psi_n|, \quad \vec{p}(t) = e^{-H_{\text{eff}}t}\vec{p}(0), \qquad (5)$$

where $\vec{p}$ is a vector of probabilities p_n. Although the generator is a "quantum" matrix, of size 2^L, it can be considered as a generator of a classical Markov process. In particular, the propagator is a stochastic matrix, $\sum_m[e^{-H_{\text{eff}}t}]_{m,n} = 1$, conserving total probability $\sum_n p_n$. H_{eff} (4), yielding evolution (5), is the main result of our work.

Even without further calculations we can draw several important consequences. Evolution with H_{eff} (4) immediately implies that the unique scaling variable for $\rho(t)$ (and all observables) is $\tau = J^2\gamma t/h^2$. Furthermore, H_{eff}, and with it dynamics for $t > 1/\gamma$, does not depend on the interaction Δ. The fact that H_{eff} is always isotropic, regardless of the interaction Δ in the original H, is due to probability conservation (anisotropic H_{eff} would not result in a stochastic propagator). There is an interesting duality: $\rho(t)$ is again governed by a disordered Hamiltonian, but this time with the disorder in bonds. Even though the distribution of bond strengths in (4) is singular, after exponentiation large eigenvalues do not contribute to $e^{-H_{\text{eff}}t}$ on times larger than $1/\gamma$ (higher order terms left out from H_{eff} would also make the strongest bond finite, see Appendix A. It is not known whether H_{eff} (4), reinterpreted as a quantum Hamiltonian, displays MBL [35,36]. Below we shall demonstrate the validity of the description with H_{eff}, in particular showing that higher order terms in the perturbation series are negligible even for not-so-large $h = 4$, that the convergence radius does not shrink with the system size, and calculate interesting physical quantities.

III. NUMERICAL RESULTS

Looking at the spectrum of $\mathcal{L}$, see Appendix A (Fig. 5), we observe that there are $\approx 2^L$ real eigenvalues, while most $\sim 4^L$ have nonzero imaginary part. The simplest way to understand such a separation is to consider a perturbation theory in γ in the unperturbed operator eigenbasis of $|\psi_m\rangle\langle\psi_n|$. The eigenvalues/eigenoperators corresponding to $m \neq n$ obtain a nonzero real part (the decay rate) in multiples of 2γ. As a consequence, the off-diagonal elements of $\rho(t)$ decay within times $t < 1/\gamma$. For $m = n$ the degeneracy of unperturbed eigenvalues 0 is lifted by the second order perturbation theory, and those are the eigenvalues of interest to us and are described by H_{eff} even for a single disorder realization, see Appendix A.

The first quantity that we study is purity $I(t) := \text{tr}\rho^2(t)$. It is simpler for analytical treatment than the von Neumann entropy $S(t) := -\text{tr}\rho(t)\log_2 \rho(t)$, and we shall demonstrate that $S(t)$ behaves in essentially the same way as $-\log_2 I(t)$. In our effective diagonal Markov description we have $I(t) = \sum_n p_n^2(t)$, and similarly for $S(t) = -\sum_n p_n(t)\log_2 p_n(t)$. Note that $S(t)$ is not a measure of quantum entanglement of $\rho(t)$ — the state is diagonal in computational basis and hence nonentangled for $t > 1/\gamma$. For the initial state we first choose the antiferromagnetic (AF) state $|\downarrow\uparrow\downarrow\uparrow\cdots\downarrow\uparrow\rangle$ also used in experiments [16]. In Fig. 1 we show a comparison between a disorder-averaged $I(t)$ calculated with the exact evolution with $\mathcal{L}$ and the one calculated using H_{eff} (4). As predicted, for $t > \frac{1}{\gamma}$ the effective description is correct, not just for the average purity, but also for fluctuations, and even for each disorder realization separately. We also see that $-\log_2 I$ is an extensive quantity as it is proportional to L. For large times, in the crossover regime to the saturation value, there is a subleading small dependence on the system size, whereas for shorter times the asymptotic behavior for $L \to \infty$ is already reached for smaller L (curves for different L overlap for $t \leqslant 50$). Even though our theory is perturbative in $1/h$, already for $h = 4$ a good agreement is achieved.
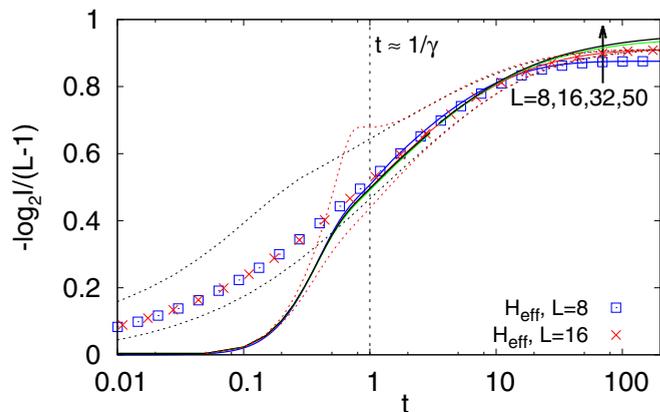
FIG. 1. Disorder-averaged purity for exact (full curves, $L = 8$ blue, 16 red, 32 green, 50 black) and approximate evolutions with H_{eff} (squares and crosses): for times larger than $t \sim \frac{1}{\gamma}$ the two agree, as well as their fluctuations due to disorder (dotted red/black lines are standard deviations $-\log_2 (I \pm \sigma)/(L - 1)$ for evolution by $\mathcal{L}$ and H_{eff}, respectively). $\mathcal{L}$ data for $L = 8$ is obtained by exact diagonalization, $L = 16, 32, 50$ with tDMRG (see Ref. [26] for details of implementation). AF initial state is used, $\gamma = J = 1$, $h = 4$, $\Delta = 0.5$.

Next, we verify the predicted scaling of the purity, which is

$$-\log_2 I(t) = (L - 1)f(\tau), \qquad \tau = \frac{J^2 \gamma t}{h^2}, \qquad (6)$$

where $f(\tau)$ is a scaling function (that can depend on the initial state). To that end we show in Fig. 2(a) the scaling function obtained from H_{eff} as well as results of exact
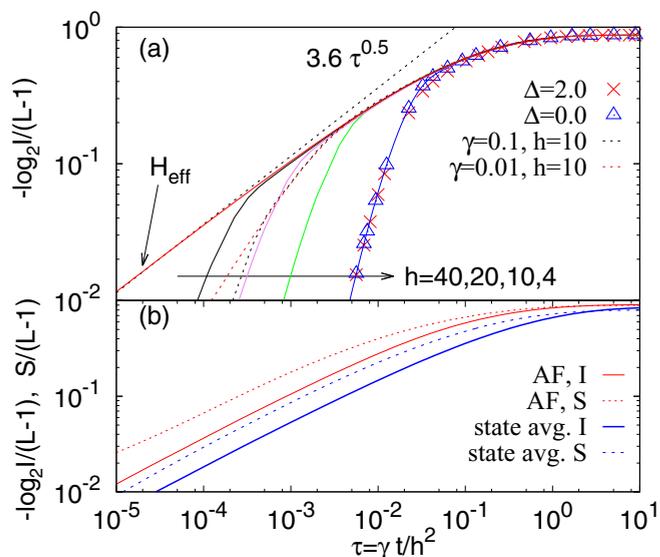

FIG. 2. (a) Purity scaling function (6) for the AF initial state (full red curve, obtained with H_{eff} and $L = 16$) and exact dynamics with $\mathcal{L}$ ($L = 8$) for different h (full curves), γ (two dotted curves) and Δ (symbols). (b) The scaling function for a disorder-averaged purity $I(t)$ (full curves) behaves essentially the same as a disorder-averaged entropy $S(t)$ (dotted curves). Red curves are for the AF initial state, blue ones for the state-averaged quantities (7) (all for H_{eff}). For all curves [in (a) and (b)], all unspecified parameters are $h = 4$, $\gamma = J = 1$, $\Delta = 0.5$.

simulation for different h, γ, and Δ, all collapsing on the scaling function [37] for $t > \frac{1}{\gamma}$. For large h there is therefore no dependence on the interaction Δ (for the XX chain with disorder and dephasing some exact results are available [38]). For small τ, which is reachable for large h, the scaling function behaves as $f(\tau) \sim \sqrt{\tau}$, explanation of which is very simple: Shortest times are dominated by largest eigenvalues of H_{eff} due to diverging bond strength (4) for resonant h_j. Considering just the strongest bond (in the spirit of real space renormalization group) giving eigenvalue $4/(h_1 - h_2)^2$, results in disorder averaging $\int dh_1 dh_2 \exp(-16t/(h_1 - h_2)^2)$. Expansion of this (exact for $L = 2$) purity results in a $\sqrt{\tau}$ behavior, which together with $L - 1$ possible (largest) bonds gives [39] $-\log_2 I \sim (L - 1)\sqrt{\tau} + \cdots$. We also calculated the state-averaged purity $\langle I(t) \rangle$, with averaging being done over all initial states $|\psi_n\rangle\langle\psi_n|$, the expression for which is a partition function of H_{eff} at inverse temperature $2t$ (Appendix B).

$$\langle I(t) \rangle = \frac{1}{2^L} \text{tr}[e^{-2H_{\text{eff}}t}]. \qquad (7)$$

$\langle I(t) \rangle$ might be more representative than $I(t)$ for the AF initial state, however, as Fig. 2(b) demonstrates, it behaves in qualitatively the same way as the AF purity. This thermodynamic nature of $I(t)$ and $S(t)$ explains extensivity of $-\log_2 I(t)$ and $S(t)$ for typical initial states, as well as the fact that there are no MBL-like signatures in $S(t)$ or $I(t)$ because thermodynamic expectation values are not able to detect an MBL phase [14,15].

While a typical initial state will result in a scaling function that does not depend on L, there can be exceptions. As an important example we take a domain wall initial state $|\uparrow \ldots \uparrow\downarrow \ldots \downarrow\rangle$ with zero total magnetization. The effective ferromagnetic H_{eff}, (4), has a global $SU(2)$ invariance, implying degeneracy. The two lowest eigenmodes (including zero) are the same in all nontrivial magnetization sectors of H_{eff} [40]. Interestingly, even with the disordered bonds the low lying excitations of a ferromagnetic H_{eff} have a magnon nature. For example, in the one-magnon sector the low-energy (real) eigenvalues of $\mathcal{L}$ are well approximated by $\lambda_j \sim \gamma J^2 j^2/(h^2 L^2)$. Numerical demonstration that the spectral gap of many-body $\mathcal{L}$ as well scales as $\propto 1/L^2$ is shown in the inset of Fig. 3. Low-energy physics of H_{eff}, and with it long time dynamics of $\mathcal{L}$, is therefore of a hydrodynamic diffusive nature. Because the domain wall initial state has a large overlap with these long wavelength modes (unlike in AF state) the time-dependence of purity gets an additional L^2 factor, with the scaling variable being $J^2 \gamma t/(hL)^2$, Fig. 3. There is again a good agreement between the full Liouvillian dynamics and the dynamics given by H_{eff}. We note that, since τ is proportional to the spectral gap of $\mathcal{L}$, such domain wall initial state could be used to experimentally measure the scaling of the gap [31] with L — a spectral quantity of fundamental importance that would be difficult to measure otherwise.

IV. NONTHERMODYNAMIC QUANTITY

So far we have been concerned with $I(t)$, which is a thermodynamic expectation value of H_{eff}, and as such can not signal any possible MBL in H_{eff}. We are now going to consider a quantity which behaves differently. If we make
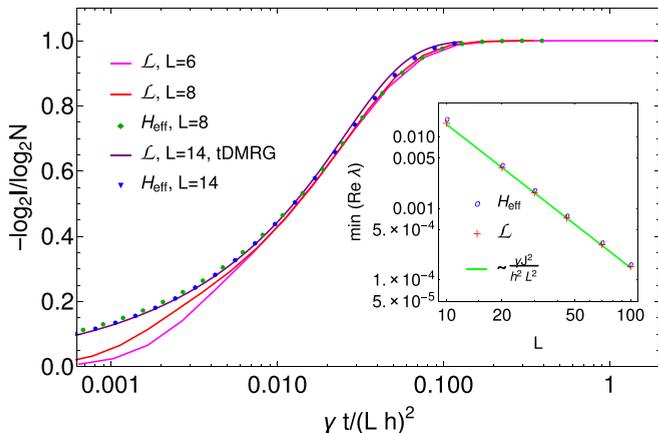
FIG. 3. Scaling function for the domain wall initial state. $N = \binom{L}{L/2}^2$ is the Hilbert space dimension of the sector with zero magnetization [41] ($h = 4, \gamma = J = 1, \Delta = 0.5$). Inset: Scaling of the largest eigenvalue of $\mathcal{L}$ (the gap) with the system size in the one-magnon sector.

a bipartition of the chain into two halves and Schmidt decompose $\rho(t)$ as $\rho(t) = \sum_k \sqrt{\mu_k} A_k \otimes B_k$, where A_k are orthogonal, $\mathrm{tr}A_k^\dagger A_p \propto \delta_{k,p}$, and similarly for B_k, and use normalization $\sum_k \mu_k = 1$, we can define the operator-space entanglement entropy (OSEE) [42] $S^\sharp := -\sum_k \mu_k \log_2 \mu_k$. It measures nonfactorizability of $\rho(t)$ (it is the entanglement entropy of $|\rho(t)\rangle$ considered as a pure state in the Hilbert space of operators). For MBL systems it has been shown that $S^\sharp(t)$ for initial localized operators grows in the same logarithmic way as $S(t)$ for pure product initial states [7]. We observe that in our effective description probabilities $\vec{p}(t)$ are evolved (5) by $e^{-H_{\mathrm{eff}}t}$ in the same way as would be a pure state in unitary evolution by H_{eff} (barring the "imaginary time"). Therefore, the OSEE $S^\sharp(t)$ could behave in a similar way as would von Neumann entropy for evolution of pure states with H_{eff}. We note that $S^\sharp$ is in fact a decisive quantity for the efficiency [43] of our tDMRG simulations of $\rho(t)$, see Fig. 4. One can observe
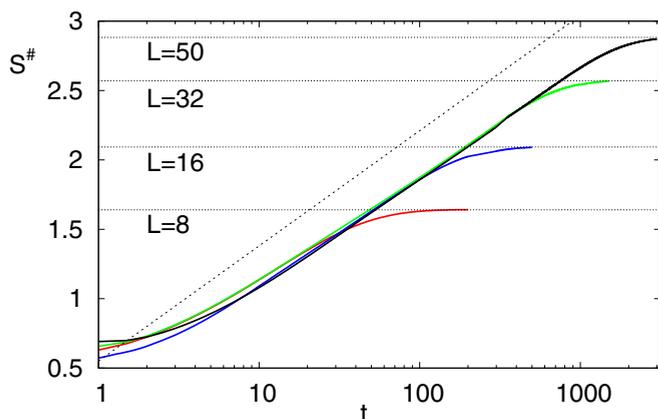

FIG. 4. Operator-space entanglement entropy $S^\sharp(t)$ of $\rho(t)$ for the exact evolution with $\mathcal{L}$ ($\gamma = J = 1, h = 4, \Delta = 0.5$) and AF initial state. Dotted black line is $\frac{1}{4}\log_2(t)$ + const., suggesting logarithmic growth. Horizontal dashed lines are the exact theoretical saturation values of $S^\sharp \propto \frac{1}{2}\log_2 L$ obtained from the steady-state Schmidt coefficients of the projection of $\mathbb{1}$ to the half-filled subspace [31].

a suggestive logarithmic growth $S^\sharp(t) \sim \frac{1}{4}\log_2(t)$ for over two decades in time, with a prefactor $\frac{1}{4}$ seemingly being equal to $\frac{1}{2\nu}$, where ν is the critical exponent of the Liouvillian gap, $g \asymp 1/L^\nu$ ($\nu = 2$ in our model). Importantly, as opposed to $S(t)$, the OSEE $S^\sharp$ is not extensive, making such logarithmic growth at all possible. Of course, for long times $S^\sharp$ saturates at the steady-state value that scales asymptotically [31] as $\frac{1}{2}\log_2[\frac{\pi e}{8}L]$, and corresponds to the trivial steady state with no MBL.

V. CONCLUSION

We have shown that the long-time dynamics of the MBL system with dephasing noise is described by an effective stochastic process generated by a bond-disordered ferromagnetic spin chain. Such description becomes more and more precise at large h and is independent in the leading order of $1/h$ from the interaction strength Δ in the Hamiltonian, explaining experimental observations [19]. The scaling variable is shown to be $\gamma t/h^2$ for all observables. The modes which survive at long times have a hydrodynamic long-range nature. The purity and von Neumann entropy at long times behave as thermodynamic quantities and do not exhibit any MBL signatures. On the other hand, the operator-space entanglement entropy, measuring factorizability in the operator space, does exhibit logarithmic growth in time. Perturbative calculation proposed could be used also for other MBL systems, including some other types of dissipation. We also discuss how, with a right choice of the initial state, one could experimentally "measure" the Liouvillian gap.

Note added in proof. After completion of this work a preprint appeared [44] studying the same model, but focusing on different physical properties.

APPENDIX A: DERIVATION OF THE EFFECTIVE EVOLUTION OPERATOR

In our derivation of the effective evolution operator H_{eff} we closely follow the Supplemental Material of Ref. [32], where a similar derivation has been done, only in the absence of the disorder in the parameters of the model. We also note that in Ref. [33] a bit different perturbative method has been used for Rydberg systems, leading in general to similar results.

The evolution operator of the open system is:

$$\mathcal{L}[\rho] = -i[H, \rho] + \mathcal{D}[\rho],$$

$$H = \sum_{j=1}^{L} J_j\left(\sigma_j^x \sigma_{j+1}^x + \sigma_j^y \sigma_{j+1}^y + \Delta_j \sigma_j^z \sigma_{j+1}^z\right) + \sum_{j=1}^{L} h_j \sigma_j^z,$$

$$\mathcal{D}[\rho] = \sum_j (2l_j \rho l_j^\dagger - \{l_j^\dagger l_j, \rho\}), \quad l_j = \sqrt{\gamma_j/2}\,\sigma_j^z.$$

Here we put periodic boundary conditions for the Hamiltonian, unlike in the main text, where open boundary conditions are used. We do it in order to have more symmetric expressions

for the couplings of the effective evolution operator. For large systems one should not expect any difference between periodic and open boundary conditions.

Perturbation expansion is performed with respect to the part of the Liouvillian which is diagonal in the z basis:

$$\mathcal{L}_0[\rho] = -i[H_Z,\rho] + \mathcal{D}[\rho],$$

$$H_Z = \sum_{j=1}^{L} J_j \Delta_j \sigma_j^z \sigma_{j+1}^z + \sum_{j=1}^{L} h_j \sigma_j^z. \tag{A1}$$

For $\mathcal{L}_0$ the nonequilibrium steady state, $\rho(t=\infty)$, has degeneracy 2^L and consists only of diagonal density matrices, $\rho_0^\kappa = |\kappa\rangle\langle\kappa|$, where $|\kappa\rangle \equiv |\psi_n\rangle$ is the nth computation basis vector in the σ_j^z eigenbasis, $|\kappa\rangle = |\sigma_1\sigma_2\ldots\sigma_L\rangle$, $\sigma_i^z|\kappa\rangle = \sigma_i|\kappa\rangle, \forall i$, and $\sigma_j = 1$ for spin up and $\sigma_j = -1$ for spin down. The degeneracy is lifted by the hopping between the sites:

$$\mathcal{L}_1[\rho] = -i[H_{XX},\rho],$$

$$H_{XX} = \sum_{j=1}^{L} J_j\big(\sigma_j^x \sigma_{j+1}^x + \sigma_j^y \sigma_{j+1}^y\big). \tag{A2}$$

The action of the $\mathcal{L}_1$ on the single diagonal density matrix ρ_0^κ is:

$$\mathcal{L}_1\rho_0^\kappa = -i\sum_j J_j(|\kappa^{(j)}\rangle\langle\kappa| - |\kappa\rangle\langle\kappa^{(j)}|), \tag{A3}$$

where $|\kappa^{(j)}\rangle = \frac{1}{2}(\sigma_j^x\sigma_{j+1}^x + \sigma_j^y\sigma_{j+1}^y)|\kappa\rangle$. So we see that the first order of the perturbation theory gives zero, as $\langle\kappa|\kappa^{(j)}\rangle = 0$, while the second order does not vanish:

$$\mathcal{L}_{\text{eff}} = -\mathcal{P}\mathcal{L}_1(1-\mathcal{P})\mathcal{L}_0^{-1}(1-\mathcal{P})\mathcal{L}_1\mathcal{P}, \tag{A4}$$

where $\mathcal{P}$ is a projector on the zero-eigenvalue subspace of $\mathcal{L}_0$:

$$\mathcal{P}[\rho] = \sum_\kappa \text{tr}(\rho\rho_0^\kappa)\rho_0^\kappa. \tag{A5}$$

$\mathcal{L}_1$ has nonzero matrix elements only in the subspace orthogonal to $\mathcal{P}$, therefore the factor $1-\mathcal{P}$ is not necessary in the expression (A4).

We notice that $|\kappa^{(j)}\rangle \neq 0$ if and only if the spins on the neighboring sites $j,j+1$ point in different directions, $\sigma_j\sigma_{j+1} = -1$. The eigenvalue of $\mathcal{L}_0$ with the eigenoperator $|\kappa^{(j)}\rangle\langle\kappa|$ is

$$\epsilon_{j,\kappa} = 2i\sigma_j(h_j - h_{j+1} + \sigma_{j-1}J_{j-1}\Delta_{j-1} - \sigma_{j+2}J_{j+1}\Delta_{j+1}) - 2(\gamma_j + \gamma_{j+1})$$

and, correspondingly, the one with eigenoperator $|\kappa\rangle\langle\kappa^{(j)}|$ is

$$\epsilon'_{j,\kappa} = -2i\sigma_j(h_j - h_{j+1} + \sigma_{j-1}J_{j-1}\Delta_{j-1} - \sigma_{j+2}J_{j+1}\Delta_{j+1}) - 2(\gamma_j + \gamma_{j+1}).$$

We notice that ϵ and ϵ' are complex conjugated. The eigenvalues ϵ and ϵ' depend on the spin projections σ_j in $|\kappa\rangle$ at positions $j, j-1, j+2$.

Now we can apply $\mathcal{P}\mathcal{L}_1$ to $\mathcal{L}_0^{-1}\mathcal{L}_1\rho_0^\kappa$:

$$-\mathcal{L}_{\text{eff}}\rho_0^\kappa = -i\frac{2J_j\mathcal{P}}{\epsilon_{j,\kappa}}[H_{XX}|\kappa^{(j)}\rangle\langle\kappa| - |\kappa^{(j)}\rangle\langle\kappa|H_{XX}] + i\frac{2J_j\mathcal{P}}{\epsilon_{j,\kappa}^*}[H_{XX}|\kappa\rangle\langle\kappa^{(j)}| - |\kappa\rangle\langle\kappa^{(j)}|H_{XX}]. \tag{A6}$$

The very first and the very last term in the expression above give a diagonal contribution:

$$\sum_j 2J_j^2\langle\kappa|\big(\sigma_j^z\sigma_{j+1}^z - 1\big)|\kappa\rangle \cdot |\kappa\rangle\langle\kappa|\left(\frac{1}{\epsilon_{j,\kappa}} + \frac{1}{\epsilon_{j,\kappa}^*}\right), \tag{A7}$$

while the other two terms change $|\kappa\rangle\langle\kappa|$ into $|\kappa^{(j)}\rangle\langle\kappa^{(j)}|$, so they can be written as

$$\sum_j 2J_j^2\langle\kappa^{(j)}|\big(\sigma_j^x\sigma_{j+1}^x + \sigma_j^y\sigma_{j+1}^y\big)|\kappa\rangle \cdot |\kappa^{(j)}\rangle\langle\kappa^{(j)}|\left(\frac{1}{\epsilon_{j,\kappa}} + \frac{1}{\epsilon_{j,\kappa}^*}\right). \tag{A8}$$

The multiplier proportional to hoppings $t_{j,\kappa}$ depends only on σ_{j-1} and σ_{j+2}:

$$t_{j,\kappa} \equiv \frac{1}{\epsilon_{j,\kappa}} + \frac{1}{\epsilon_{j,\kappa}^*} = -\frac{(\gamma_j + \gamma_{j+1})}{(h_j - h_{j+1} + \sigma_{j-1}J_{j-1}\Delta_{j-1} - \sigma_{j+2}J_{j+1}\Delta_{j+1})^2 + (\gamma_j + \gamma_{j+1})^2}. \tag{A9}$$

In total the effective evolution operator is:

$$\mathcal{L}_{\text{eff}}|\kappa\rangle\langle\kappa| = \sum_j \sum_{\kappa^{(j)}} 2J_j^2 t_{j,\kappa}\langle\kappa^{(j)}|(1 - \vec{\sigma}_j \cdot \vec{\sigma}_{j+1})|\kappa\rangle|\kappa^{(j)}\rangle\langle\kappa^{(j)}|. \tag{A10}$$

Depending on the sign of the spin projection at the positions $j-1$ and $j+2$ there are two possibilities for signs between $J_{j-1}\Delta_{j-1}$ and $J_{j+1}\Delta_{j+1}$: If the spins at the sites $j-1$ and $j+2$ have the same direction, then the sign is minus, while otherwise plus. Therefore, $\mathcal{L}_{\text{eff}}|\kappa\rangle\langle\kappa|$ can be also rewritten explicitly as the sum over projectors onto different neighboring spin-configurations:

$$\mathcal{L}_{\text{eff}}|\kappa\rangle\langle\kappa| = \sum_{\kappa'}\langle\kappa'|H_{\text{eff}}|\kappa\rangle \cdot |\kappa'\rangle\langle\kappa'|, \tag{A11}$$

$$H_{\text{eff}} = \frac{1}{4}\sum_j \sum_{\alpha,\beta=+,-} T_{j,\alpha\beta}\big(1 + \alpha\sigma_{j-1}^z\big)\big(1 - \vec{\sigma}_j \cdot \vec{\sigma}_{j+1}\big)\big(1 + \beta\sigma_{j+2}^z\big), \alpha,\beta = +,-, \tag{A12}$$

$$T_{j,\alpha\beta} = \frac{2J_j^2(\gamma_j + \gamma_{j+1})}{(h_j - h_{j+1} + \alpha J_{j-1}\Delta_{j-1} - \beta J_{j+1}\Delta_{j+1})^2 + (\gamma_j + \gamma_{j+1})^2}. \tag{A13}$$

This form underlines the nonlocal structure of the effective evolution operator.

The matrix H_{eff} has the following property:

$$\forall k \in \mathbb{N} : \sum_m \left(H_{\text{eff}}^k\right)_{mn} = 0, \quad \sum_n \left(H_{\text{eff}}^k\right)_{mn} = 0, \tag{A14}$$

therefore $\exp(-H_{\text{eff}}t)$ is a doubly stochastic matrix, i.e., $\sum_m \exp(-H_{\text{eff}}t)_{mn} = 1$ as well as $\sum_n \exp(-H_{\text{eff}}t)_{mn} = 1$.

Disorder in magnetic field. Let us consider a case in which we are interested in the main text of the paper, namely when $h_i \in [-2h, 2h]$ and h is the largest energy scale of the problem, γ_i, $J_i \equiv J$, $J_i\Delta_i \ll h$. Then we could have naively made a Taylor expansion of the coefficients $T_{j,\alpha\beta}$ with respect to the large parameter h. However, this procedure is not well defined from the mathematical point of view as the difference $(h_j - h_{j+1})$ is a random variable, with the distribution function nonzero everywhere at the segment $[-4h, 4h]$, i.e., there can be also very small values of $(h_j - h_{j+1})$, so the Taylor expansion is not justified. In order to have a well-defined mathematical procedure for the large h expansion, we should consider a distribution function for the couplings $T_{j,\alpha\beta}$:

$$P_{\text{full}}(Y = T_{j,\alpha\beta}) = \left[P\left(x = \sqrt{\frac{2b_j J^2}{Y} - b_j^2} - \mu_j\right) + P\left(x = -\sqrt{\frac{2b_j J^2}{Y} - b_j^2} - \mu_j\right) \right] \left(\frac{Y^2}{J^2 b_j}\sqrt{\frac{2b_j J^2}{Y} - b_j^2}\right)^{-1}, \tag{A15}$$

$$P(x) = \begin{cases} \frac{4h-x}{4h}, & x \geqslant 0, \\ \frac{4h+x}{4h}, & x < 0, \end{cases} \tag{A16}$$

$$b_j = \gamma_j + \gamma_{j+1}, \quad \mu_j = \sigma_{j-1}\Delta_{j-1}J - \sigma_{j-2}\Delta_{j+1}J. \tag{A17}$$

Compare this with the distribution function for the couplings $T_{j,\alpha\beta}$ which we would have obtained had we performed a naive Taylor expansion:

$$P_0\left(Y = \frac{2b_j J^2}{(h_j - h_{j+1})^2}\right) = J\sqrt{2b_j}\frac{4h\sqrt{Y} - J\sqrt{2b_j}}{(4h)^2 Y^2}. \tag{A18}$$

We see that we obtain P_0 from P_{full} for $h \gg \mu_j$ and $\frac{J^2}{Y} \gg b_j$. The first inequality requires the interaction Δ to be small comparing to the disorder strength h. The second inequality is rewritten as $Y \ll \frac{J^2}{\gamma}$ as well as we expect that $Y \leqslant \frac{\gamma J^2}{h^2}$, which gives us a condition $\gamma \ll h$ (here we assumed for simplicity $\gamma_j \equiv \gamma$).

The terms containing more than two spins, e.g., $\sigma_{j-1}^z(1 - \vec{\sigma}_j\vec{\sigma}_{j+1})\sigma_{j+2}^z$, are canceled in this order of the expansion (the condition $\Delta \ll h$ is important for such cancellation), so we arrive at H_{eff} given in the main text.

Let us note that the two distributions, $P_{\text{full}}(Y)$ and $P_0(Y)$, have significantly different behavior for $Y \to \infty$: while $P_{\text{full}}(Y) = 0$, for $Y > b_j^2/J^2$, $P_0(Y)$ has an infinite tail $P_0(Y) \propto Y^{-3/2}$. However, as we are interested in the long time dynamics of the propagator $e^{-H_{\text{eff}}t}$, which is driven mostly by the small eigenvalues of H_{eff}, and therefore small J_{eff}, the largest eigenvalues of H_{eff}, which are given by the tail of the distribution $P(Y)$, $Y \to \infty$, are not important.

Let us note that in the one magnon sector, i.e., for H_{eff} restricted to a Hilbert subspace with a single overturned spin, there is no dependence on Δ at all.

Disorder in the interaction strength. We can also deduce from Eq. (A12) that at $h_i = 0$ and disorder in Δ_j, $\Delta_j \in [-\Delta, \Delta]$, $\Delta \gg 1$, the effective evolution operator is not reducible to the nearest spin interaction only and contains also four spin terms. We notice as well that our effective evolution

operator can be used also for describing the dynamics in more than one dimension, as dimensionality of the lattice has not been used in the derivation.

Numerical comparison of the spectrum

Here we show, see Fig. 5, the full spectrum of $\mathcal{L}$ and compare its real eigenvalues with the spectrum of H_{eff}. The spectrum of $\mathcal{L}$ contains 4^L eigenvalues. The eigenvalues which determine the long-time dynamics are in clear correspondence with the eigenvalues of H_{eff} given in the text.

APPENDIX B: AVERAGING PURITY OVER THE STATES

In this section we explicitly show the connection between the purity and the statistical sum of the effective evolution
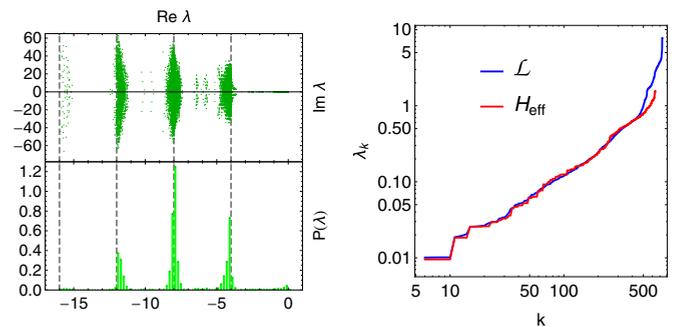

FIG. 5. Left: The spectrum of the Liouvillian for $L = 8$ (in the largest sector where bra and ket have the same magnetization). Lower frame shows the density of real parts of eigenvalues. Right: Comparison of the spectra of H_{eff} and of purely real eigenvalues of $\mathcal{L}$ for $L = 10$. Parameters are $h = 4$, $\gamma = 1$, $J = 0.5$, $\Delta = 1.0$.

operator. The purity is defined as

$$I(t) = \mathrm{tr}\rho^2(t). \tag{B1}$$

Let us express it in terms of the spectral form of H_{eff}:

$$H_{\mathrm{eff}} = \sum_n \lambda_n |\phi_n\rangle\langle\phi_n|. \tag{B2}$$

On the other side, as $\mathcal{L}_{\mathrm{eff}}$ acts in the space of the diagonal density matrices, so that the purity is

$$I(t) = \sum_n p_n^2(t), \tag{B3}$$

where p_n is the nth component of the probability vector which evolves as

$$|p(t)\rangle = \sum_n e^{-\lambda_n t} |\phi_n\rangle\langle\phi_n|p(0)\rangle. \tag{B4}$$

So it follows that

$$\sum_n p_n^2(t) = \sum_n \left(\sum_{j_1} e^{-\lambda_{j_1} t} \langle\phi_{j_1}|p(0)\rangle\langle\psi_n|\phi_{j_1}\rangle \right)$$
$$\times \left(\sum_{j_2} e^{-\lambda_{j_2} t} \langle\phi_{j_2}|p(0)\rangle\langle\psi_n|\phi_{j_2}\rangle \right). \tag{B5}$$

If we separate H_{eff} into different magnetization sectors then in each of the sectors eigenvalues are nondegenerate, positive, the operator itself has only real values, so its eigenvectors $|\phi_j\rangle$ have only real entries $\langle\psi_n|\phi_j\rangle$, therefore orthogonality condition between different vectors can be written without complex conjugation:

$$\langle\phi_{j_1}|\phi_{j_2}\rangle = \delta_{j_1 j_2} \Rightarrow \sum_n \langle\psi_n|\phi_{j_1}\rangle\langle\psi_n|\phi_{j_2}\rangle = \delta_{j_1 j_2}. \tag{B6}$$

Hence the purity for the initial density matrix which has only diagonal elements, and therefore is described by the probability vector $|p(0)\rangle$, can be written as

$$I(t) = \sum_j e^{-2\lambda_j t} |\langle\phi_j|p(0)\rangle|^2. \tag{B7}$$

The purity averaged over initial states in the whole Hilbert space of H_{eff} is

$$\langle I(t)\rangle_{\mathcal{H}_{\mathrm{eff}}} = \frac{1}{\dim H_{\mathrm{eff}}} \sum_{j=1}^{\dim H_{\mathrm{eff}}} e^{-2\lambda_j t} \equiv \frac{\mathrm{tr}\exp(-2H_{\mathrm{eff}}t)}{\dim H_{\mathrm{eff}}},$$

$$\mathrm{as}\langle|\langle\phi_j|p(0)\rangle|^2\rangle_{H_{\mathrm{eff}}} = \frac{1}{\dim H_{\mathrm{eff}}}. \tag{B8}$$

The dimension of the effective evolution operator $\dim H_{\mathrm{eff}}$ equals to the dimension of the fixed magnetization (particle number) sector under consideration.

---

[1] P. W. Anderson, Absence of diffusion in certain random lattices, Phys. Rev. **109**, 1492 (1958).

[2] J. M. Deutsch, Quantum statistical mechanics in a closed system, Phys. Rev. A **43**, 2046 (1991).

[3] I. V. Gornyi, A. D. Mirlin, and D. G. Polyakov, Interacting Electrons in Disordered Wires: Anderson Localization and Low-T Transport, Phys. Rev. Lett. **95**, 206603 (2005).

[4] D. M. Basko, I. L. Aleiner, and B. L. Altschuler, Metal-insulator transition in a weakly interacting many-electron system with localized single-particle states, Ann. Phys. **321**, 1126 (2006).

[5] V. Oganesyan and D. A. Huse, Localization of interacting fermions at high temperature, Phys. Rev. B **75**, 155111 (2007).

[6] R. Vosk and E. Altman, Dynamical Quantum Phase Transitions in Random Spin Chains, Phys. Rev. Lett. **112**, 217204 (2014).

[7] M. Žnidarič, T. Prosen, and P. Prelovšek, Many-body localization in the Heisenberg XXZ magnet in a random field, Phys. Rev. B **77**, 064426 (2008).

[8] J. H. Bardarson, F. Pollmann, and J. E. Moore, Unbounded Growth of Entanglement in Models of Many-Body Localization, Phys. Rev. Lett. **109**, 017202 (2012).

[9] D. A. Huse, R. Nandkishore, and V. Oganesyan, Phenomenology of fully many-body-localized systems, Phys. Rev. B **90**, 174202 (2014).

[10] M. Serbyn, Z. Papić, and D. A. Abanin, Local Conservation Laws and the Structure of the Many-Body Localized States, Phys. Rev. Lett. **111**, 127201 (2013).

[11] V. Ros, M. Müller, and A. Scardicchio, Integrals of motion in the many-body localized phase, Nucl. Phys. B **891**, 420 (2015).

[12] J. Z. Imbrie, arXiv:1403.7837.

[13] A. Pal and D. A. Huse, Many-body localization phase transition, Phys. Rev. B **82**, 174411 (2010).

[14] R. Nandkishore and D. A. Huse, Many-body localization and thermalization in quantum statistical mechanics, Annu. Rev. Condens. Matter Phys. **6**, 15 (2015).

[15] E. Altman and R. Vosk, Universal dynamics and renormalization in many-body-localized systems, Annu. Rev. Condens. Matter Phys. **6**, 383 (2015).

[16] M. Schreiber, S. S. Hodgman, P. Bordia, H. P. Lüschen, M. H. Fischer, R. Vosk, E. Altman, U. Schneider, and I. Bloch, Observation of many-body localization of interacting fermions in a quasi-random optical lattice, Science **349**, 842 (2015).

[17] J. Smith, A. Lee, P. Richerme, B. Neyenhuis, P. W. Hess, P. Hauke, M. Heyl, D. A. Huse, and C. Monroe, arXiv:1508.07026.

[18] P. Bordia, H. P. Lüschen, S. S. Hodgman, M. Schreiber, I. Bloch, and U. Schneider, arXiv:1509.00478.

[19] U. Schneider, private discussion; I. Bloch and H. P. Lüschen, KITP conference talk (2015).

[20] R. Nandkishore, S. Gopalakrishnan, and D. A. Huse, Spectral features of a many-body-localized system weakly coupled to a bath, Phys. Rev. B **90**, 064203 (2014).

[21] S. Johri, R. Nandkishore, and R. N. Bhatt, Numerical Study of a Many-Body Localized System Coupled to a Bath, Phys. Rev. Lett. **114**, 117401 (2015).

[22] K. Hyatt, J. R. Garrison, A. C. Potter, and B. Bauer, arXiv:1601.07184.

[23] C. W. Gardiner and P. Zoller, *Quantum Noise*, 1st ed. (Springer, Berlin, 1991), Ch.3.6, p. 77.

[24] H.-P. Breuer and F. Petruccione, *The Theory of Open Quantum Systems*, Ch. 3.5, p. 166 (Oxford University Press, Oxford, 2002).

[25] S. Sarkar, S. Langer, J. Schachenmayer, and A. J. Daley, Light scattering and dissipative dynamics of many fermionic atoms in an optical lattice, Phys. Rev. A **90**, 023618 (2014).

[26] M. Žnidarič, Dephasing-induced diffusive transport in the anisotropic Heisenberg model, New J. Phys. **12**, 043001 (2010).

[27] E. Levi, M. Heyl, I. Lesanovsky, and J. P. Garrahan, arXiv:1510.04634.

[28] A. Carmele, M. Heyl, C. Kraus, and M. Dalmonte, Stretched exponential decay of Majorana edge modes in many-body localized Kitaev chains under dissipation, Phys. Rev. B. **92**, 195107 (2015).

[29] V. Gorini, A. Kossakowski, and E. C. G. Sudarshan, Completely positive dynamical semigroups of N-level systems, J. Math. Phys. **17**, 821 (1976); G. Lindblad, On the generators of quantum dynamical semigroups, Commun. Math. Phys. **48**, 119 (1976).

[30] D. J. Luitz, N. Laflorencie, and F. Alet, Many-body localization edge in the random-field Heisenberg chain, Phys. Rev. B **91**, 081103(R) (2015).

[31] M. Žnidarič, Relaxation times of dissipative many-body quantum systems, Phys. Rev. E **92**, 042143 (2015).

[32] Z. Cai and T. Barthel, Algebraic Versus Exponential Decoherence in Dissipative Many-Particle Systems, Phys. Rev. Lett. **111**, 150403 (2013).

[33] I. Lesanovsky and J. P. Garrahan, Kinetic Constraints, Hierarchical Relaxation, and Onset of Glassiness in Strongly Interacting and Dissipative Rydberg Gases, Phys. Rev. Lett. **111**, 215305 (2013).

[34] The effective H_{eff} (4) is correct in the limit of large h, keeping other parameters (Δ, γ) fixed. Other limits, for instance, letting $\gamma \to 0$ while keeping other parameters fixed will likely require a different description.

[35] K. Agarwal, E. Demler, and I. Martin, $1/f^\alpha$ noise and generalized diffusion in random Heisenberg spin systems, Phys. Rev. B **92**, 184203 (2015).

[36] R. Vasseur, A. J. Friedman, S. A. Parameswaran, and A. C. Potter, arXiv:1510.04282.

[37] We note that there is no logarithmic growth in time of $-\log_2 I$ (or $S(t)$) as $f(\tau) \in [0,1]$, whereas the logarithm has the whole positive real axis for its range.

[38] M. Žnidarič and M. Horvat, Transport in a disordered tight-binding chain with dephasing, Eur. Phys. J. B **86**, 67 (2013).

[39] For a single disorder realization, where the largest bond is finite, for times smaller than this inverse energy, dependence is $-\log I \sim \tau$, leading to $\sim \sqrt{\tau}$ behavior only after disorder averaging.

[40] T. Koma and B. Nachtergaele, The spectral gap of the ferromagnetic XXZ-chain, Lett. Math. Phys. **40**, 1 (1997).

[41] In Fig. 3 we scale the purity with the exact dimension of the Hilbert space. In the thermodynamic limit the factor $\log_2 N$ and $L - 1$ used in other figures coincide.

[42] T. Prosen and I. Pižorn, Operator space entanglement entropy in transverse Ising chain, Phys. Rev. A **76**, 032316 (2007).

[43] T. Prosen and M. Žnidarič, Is the efficiency of classical simulations of quantum dynamics related to integrability?, Phys. Rev. E **75**, 015202 (2007).

[44] M. H. Fischer, M. Maksymenko, and E. Altman, arXiv:1512.02669.